Biomedicine & Pharmacotherapy 93 (2017) 931–938

Available online at
ScienceDirect
www.sciencedirect.com

Elsevier Masson France
EM|consulte
www.em-consulte.com/en

Detection of bacterial infection by a technetium-99m-labeled peptidoglycan aptamer

Iêda Mendes Ferreira[a], Camila Maria de Sousa Lacerda[a], Sara Roberta dos Santos[a], André Luís Branco de Barros[b], Simone Odília Fernandes[b], Valbert Nascimento Cardoso[b], Antero Silva Ribeiro de Andrade[a,*]

[a] Centro de Desenvolvimento da Tecnologia Nuclear (CDTN), Rua Professor Mário Werneck S/N°, Cidade Universitária, Campus da UFMG, 31120-970, Belo Horizonte, MG, Brazil
[b] Departamento de Análises Clínicas e Toxicológicas, Faculdade de Farmácia, Universidade Federal de Minas Gerais, Cidade Universitária, Campus da UFMG, 31270-091, Belo Horizonte, MG, Brazil

ARTICLE INFO

Article history:
Received 1 June 2017
Received in revised form 5 July 2017
Accepted 5 July 2017

Keywords:
Aptamer
Peptidoglycan
Technetium-99m
Diagnosis
Bacterial infection
Radiopharmaceutical

ABSTRACT

Nuclear medicine clinicians are still waiting for the optimal scintigraphic imaging agents capable of distinguishing between infection and inflammation, and between fungal and bacterial infections. Aptamers have several properties that make them suitable for molecular imaging. In the present study, a peptidoglycan aptamer (Antibac1) was labeled with ^{99m}Tc and evaluated by biodistribution studies and scintigraphic imaging in infection-bearing mice. Labeling with ^{99m}Tc was performed by the direct method and the complex stability was evaluated in saline, plasma and in the molar excess of cysteine. The biodistribution and scintigraphic imaging studies with the ^{99m}Tc-Antibac1 were carried out in two different experimental infection models: Bacterial-infected mice (*S. aureus)* and fungal-infected mice (*C. albicans*). A ^{99m}Tc radiolabeled library, consisting of oligonucleotides with random sequences, was used as a control for both models. Radiolabeling yields were superior to 90% and ^{99m}Tc-Antibac1 was highly stable in presence of saline, plasma, and cysteine up to 6 h. Scintigraphic images of *S. aureus* infected mice at 1.5 and 3.0 h after ^{99m}Tc-Antibac1 injection showed target to non-target ratios of 4.7 ± 0.9 and 4.6 ± 0.1, respectively. These values were statistically higher than those achieved for the ^{99m}Tc-library at the same time frames (1.6 ± 0.4 and 1.7 ± 0.4, respectively). Noteworthy, ^{99m}Tc-Antibac1 and ^{99m}Tc-library showed similar low target to non-target ratios in the fungal-infected model: 2.0 ± 0.3 and 2.0 ± 0.6 for ^{99m}Tc-Antibac1 and 2.1 ± 0.3 and 1.9 ± 0.6 for ^{99m}Tc-library, at the same times. These findings suggest that the ^{99m}Tc-Antibac1 is a feasible imaging probe to identify a bacterial infection focus. In addition, this radiolabeled aptamer seems to be suitable in distinguishing between bacterial and fungal infection.

1. Introduction

If detected early, most infections can be cured with proper treatment, but a delayed diagnosis is associated with higher mortality. The sensitivity of nuclear medicine imaging techniques makes it a suitable tool for specific diagnosis of focal infections. One advantage of these techniques is the whole-body imaging, which is important when there are no localizing signs. Indications for the use of nuclear medicine imaging of infections include suspected infections in immunocompromised patients, suspected infection of a vascular implant, osteomyelitis, disk-space infection, fever of unknown origin, a suspected occult abscess and post-operative infection [1]. A variety of radiopharmaceuticals is used to detect infection, but long-term clinical use has shown that most of them cannot distinguish between inflammation and infection. Nuclear medicine clinicians are still awaiting scintigraphic imaging agents capable of distinguishing between infection and inflammation, and between fungal and bacterial infections [2].

Acid nucleic aptamers are single-stranded DNA or RNA oligonucleotides that bind to target molecules with high affinity and specificity. They are selected by an *in vitro* selection process termed SELEX (Systematic Evolution of Ligands by EXponential Enrichment) through repeated rounds of partitioning and

* Corresponding author.
E-mail addresses: imendesf@yahoo.com.br (I.M. Ferreira), cmslacerda@gmail.com (C.M. de Sousa Lacerda), sararoberta7@hotmail.com (S.R. dos Santos), brancodebarros@yahoo.com.br (A.L.B. de Barros), simone@farmacia.ufmg.br (S.O. Fernandes), valbertncardoso@gmail.com (V.N. Cardoso), antero@cdtn.br (A.S.R. de Andrade).

http://dx.doi.org/10.1016/j.biopha.2017.07.017
0753-3322/

amplification from large random synthetic oligonucleotide acid library [3,4]. Aptamers can be labeled with different radioisotopes and possess several properties that make them suitable for molecular imaging. Since their discovery, several aptamers have been used as targeting molecule of radiopharmaceuticals in preclinical studies, mainly for cancer imaging [5].

Peptidoglycan is the only cell wall polymer common to both Gram-positive and Gram-negative bacteria. It is present as a macromolecular net that coats the entire cell in combination with other substances and two components, *N*-acetylglucosamine (NAG) and *N*-acetylmuramic acid (NAM), that alternate to form the carbohydrate polymer. Thus, peptidoglycan is a lattice of glycan chains connected by multiple peptide cross-links. The particular composition of peptidoglycan makes it a possible target for specific bacterial recognition. In a previous study, we selected through SELEX two peptidoglycan aptamers termed Antibac1 and Antibac2. The binding *in vitro* of the peptidoglycan aptamers to *Staphylococcus aureus* (Gram-positive) and *Escherichia coli* (Gram-negative) cells was significantly higher than to *Candida albicans* and human fibroblasts, demonstrating their specificity to bacterial cells [6]. Taking into account the lack of specific probes for bacterial detection, aptamers as Antibac1 and Antibac2 may open an avenue for generating new radiopharmaceuticals in this field. Herein, we describe the preparation of ^{99m}Tc-Antibac1 and its application as a scintigraphic imaging probe for bacterial infection identification.

2. Material and methods

2.1. Chemical

The aptamer Antibac1 (5′TCGCGCGAGTCGTCT GGGGACAGGGAGTGCGCTGCTCCCCCCGCACGTCCTCCC 3′) previously selected by Ferreira et al. [6], was synthesized by Integrated DNA Technologies (IDT) with the introduction at the 3′end of an amino group with a 6 carbons spacer and at the 5′ end of an inverted thymidine. The ^{99m}Tc was obtained from a molybdenum generator (IPEN/Brazil). All reagents, including tricine, ethylenediamine-N', N'-diacetic acid (EDDA), $SnCl_2{\cdot}2H_2O$ were purchased from Sigma-Aldrich (São Paulo, Brazil). All other chemicals and reagents used were of analytical grade.

2.2. Microorganisms

Staphylococcus aureus (ATCC 25923) and *Candida albicans* (ATCC 18804) were cultured on BHI solid (Himedia Laboratories Pvt Ltd.) in Petri dishes at 37 °C and sub-cultured every seven days.

2.3. Animals

All protocols were approved by the local Ethics Committee for Animal Experimentation of the Federal University of Minas Gerais (CEUA/UFMG), Protocol n° 108/2014. The Swiss mice were kept in cages with wood shavings, water and common food (ad libitum) in ordinary shelves. The mice infected with *C. albicans* were firstly immunosuppressed by gamma radiation in a uniform ^{60}Co source at the Gamma Irradiation Laboratory of the Center of Nuclear Technology Development (CDTN, Brazil). A dose of 2.5 Gy and a dose rate of 75 Gy/h were used. After irradiation, the animals were maintained in autoclaved cages with wood shavings, water and food (ad libitum). Swiss mice were supplied by the School of Pharmacy, Federal University of Minas Gerais, Belo Horizonte, Brazil.

2.4. Radiolabeling procedure and radiochemical purity evaluation

The aptamer was radiolabeled with ^{99m}Tc as previously described by Correa et al. [7]. Briefly, 111.6 μmol of tricine and 28.3 μmol of EDDA were added to 300 μL of 0.9% saline. Then, 10 μL of Antibac1 aptamer (200 pmol/μL) followed by 100 μL of $SnCl_2{\cdot}2H_2O$ (8.9 mM in HCl 0.25 N) were added to the solution. The pH was adjusted to 7.0 with 1.0 M NaOH. The bottle was sealed and vacuum was applied with a syringe. The activity of 296 MBq of a ^{99m}Tc-pertechnetate solution (Na^{99m}-TcO_4^-) was added. Then, the solution was boiled in water bath for 15 min and afterward cooled in running water. The injected activity for each animal was 14.8 MBq.

The radiolabeling yield was assessed by ascending instant thin-layer chromatography (TLC) using silica gel-coated fiberglass sheets and two solvent systems: (1) 100% acetone to determine the percentage of TcO_4^- and (2) 0.9% NaCl solution with 5% NH_4OH to determine the percentage of TcO_2. The labeled product (^{99m}Tc-Antibac1) remained at the point of application when 100% acetone was used as the mobile phase (Rf = 0) and the labeled product was moved with the solvent front when 0.9% NaCl solution with 5% NH_4OH was the mobile phase (Rf = 1). The radiolabel yield was determined according to the following equation:

$$\text{Radiolabeling yield (\%)} = 100 - (\%\ TcO_4^- + \%\ TcO_2)$$

2.5. Stability of ^{99m}Tc-labeled aptamer

The stability of ^{99m}Tc-Antibac1 complex was evaluated in presence of saline, plasma and cysteine by TLC. Saline and plasma stabilities were performed by adding 100 μL of the ^{99m}Tc-Antibac1 solution in a tube containing 1.1 mL of 0.9% NaCl or fresh mice plasma. The resulting mixtures were stored at room temperature for saline and at 37 °C for plasma. Stability in the presence of cysteine was accessed by adding a 50 fold molar-excess of cysteine to the ^{99m}Tc-Antibac1 solution. To 100 μL of the radiolabeled product, 1.1 mL of cysteine solution was joined and the mixture was kept at room temperature. All solutions were analyzed at 5 min, 1 h, 3 h, 6 h and 24 h after incubation by TLC.

2.6. Evaluation of ^{99m}Tc-Antibac1 binding to plasma proteins

A blood sample (6 mL) was collected from Swiss mice and the plasma fraction was separated by centrifugation (700*g*). EDTA (0.1 M) was used as an anticoagulant. Aliquots (triplicate) of 50 μL of plasma were incubated with the radiolabeled aptamer at 37 °C for 1 and 3 h. Afterward, 1.5 mL of acetonitrile was added into each tube. The soluble and insoluble plasma fractions were separated by centrifugation and the radioactivity associated with each fraction was measured in a gamma counter.

2.7. Blood clearance

The ^{99m}Tc-Antibac1 (3.0 MBq) was administrated in Swiss mice (n = 6) through the tail vein. A small incision was made in the distal tail to enable rapid and reliable blood collection. Blood samples (20 μL) were collected at 5, 10, 15, 30, 60, 90, 120, and 240 min after administration. The samples were weighted and the radioactivity was measured in a gamma counter. The percentage of injected activity per gram (%ID/g) and the mean ± SD in each sample were determined. The data were plotted as a function of time and blood clearance analysis was performed using GraphPad PRISM version 5.01 software. The distribution half-life and elimination half-life were calculated using non-linear regression.

2.8. Biodistribution and scintigraphic imaging

Groups of six Swiss mice (20–25 g) were used (n = 6). The animals were anesthetized with a mixture of xylazine (15 mg/kg)

Table 1
In *vitro* stability of the ^{99m}Tc-Antibac1 complex in the presence of 0.9% saline, plasma, and a molar excess of cysteine (% radiolabeled yield).

Time	Saline	Plasma	Cys 50:1
5 min	95.50 ± 1.07	93.87 ± 0.21	96.09 ± 0.14
1 h	92.49 ± 2.09	97.49 ± 0.09	72.48 ± 1.00
3 h	92.93 ± 0.19	97.81 ± 0.04	73.09 ± 1.00
6 h	87.00 ± 0.43	97.34 ± 0.26	71.89 ± 0.61
24 h	93.11 ± 0.29	94.41 ± 1.48	48.88 ± 2.33

Cys, Cysteine.

and ketamine (80 mg/kg). The mice were infected intramuscularly in the right thigh with 1×10^6 cells of *S. aureus* (ATCC 25923) suspended in 100 μL of saline or infected in the same way with 1×10^5 cells of *C. albicans* (ATCC 18804). Yeast cells were used in smaller amounts since they are much larger than bacterial cells. The animals from the *C. albicans* group were immunosuppressed before infection as aforementioned (Section 2.3). A visible swelling was observed on the infected thigh of all animals 24 h after the intervention. Then, 100 μL (14.8 MBq) of the radiotracer solution (specific activity of 55.5 ± 8.3 MBq/nmol) were injected into the tail vein in each animal. The animals were anesthetized by intraperitonial injection and placed in the prone position on a γ-camera equipped with a low-energy collimator (Nuclide TH 22, Mediso, Hungary). Five minutes static planar images were acquired using a 256 x 256-pixel matrix. The images were acquired at 1.5 and 3.0 h after radiotracer injection. The scintigraphic images were analyzed in the automatic regions of interest (ROI) drawn around the infected right tight (target) which were copied to the contralateral non-infected left tight (non-target). The ratios of the count in the target ROI to non-target ROI were calculated using the total counts. The mice were euthanized 3.0 h after injection and tissue samples were dissected, weighed and their activities measured in a gamma counter. The results were expressed as the percentage of injected dose per gram of tissue (%ID/g). Target to non-target (T/NT) ratios were obtained from the analysis of radiation measured in the infected right thigh muscle in relation to radiation measured in the left thigh muscle. At the time of euthanasia, samples from infection foci were collected for microbial culture. Only animals that tested positive were considered in the study.

2.9. Statistical analysis

All data were expressed as mean ± SD and they were analyzed by GraphPad PRISM version 5.01 software. The analysis of variance (ANOVA) with a confidence interval of 95% and Tukey multiple comparison test were used. A P value < 0.05 was considered to indicate a statistically significant difference.

3. Results

3.1. Radiolabeling with ^{99m}Tc and complex stability evaluation

The Antibac1 was labeled with ^{99m}Tc by the direct method according to Correa et al. (2014) [7] leading to radiolabel yields over to 90%. The *in vitro* stability of the ^{99m}Tc-Antibac1 complex was evaluated in the presence of saline, at room temperature, and plasma at 37 °C. In addition, stability was also tested by transchelation assay towards cysteine (1:50 molar ratio). Aliquots were taken at 5 min, 1 h, 3 h, 6 h and 24 h after incubation and analyzed by TLC as above mentioned. A high complex stability was verified in presence of saline and plasma. In presence of cysteine, a reasonable stability was achieved up to 6 h, but about 51% of transchelation was verified 24 h post-incubation (Table 1). These results indicated that ^{99m}Tc-Antibac1 is stable up to 6 h and

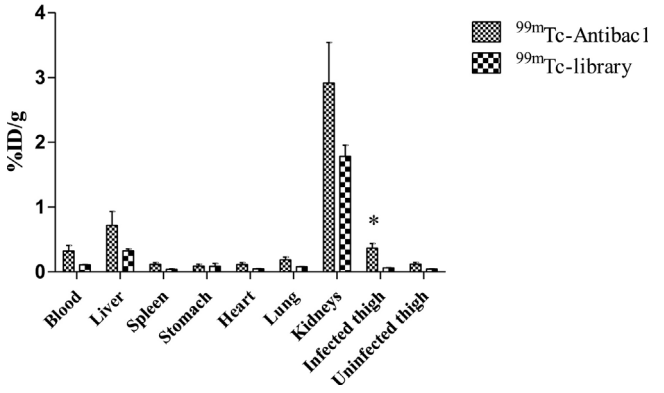

Fig. 1. ^{99m}Tc-Antibac1 and ^{99m}Tc-library biodistribution in the *S. aureus* infection model.
The Antibac1 and the library were labeled with ^{99m}Tc and injected into the tail vein. The mice (n = 6) were euthanized at 3 h after injection, tissue samples were dissected and their activities were measured in a gamma counter. The symbol (*) indicates a statistical difference in the radiation uptake between the infected right thigh and the uninfected left thigh ($p < 0.05$).

suitable for further *in vivo* assays. Interestingly, other aptamers labeled with ^{99m}Tc, reported by our group, have shown superior stability (up to 24 h) [7–9]. However, ^{99m}Tc-Antibac1 was used for early images (3 h after injection) that will not be affected by the long-term lack of stability.

3.2. Evaluation of ^{99m}Tc-Antibac1 binding to plasma proteins

The ^{99m}Tc-Antibac1 binding to plasma proteins was evaluated by incubating the radiolabeled aptamer with Swiss mouse plasma and precipitating the protein fraction using acetonitrile. The mean binding of ^{99m}Tc-Antibac1 to the insoluble fraction was of 39.5 ± 2.9 at 1 h and 43.6 ± 1.2 at 3 h, showing that the ^{99m}Tc-Antibac1 is prone to binding to plasma proteins.

3.3. Biodistribution, blood clearance, and scintigraphic imaging

The biodistribution and images of ^{99m}Tc-Antibac1 were carried out in two different experimental infection models: Bacterial-infected mice (*S. aureus*) and fungal-infected mice (*C. albicans*). A ^{99m}Tc-library, consisting of oligonucleotides in similar size of Antibac1, but with random sequences, was used as a control in both experimental models. These oligonucleotides without specificity for the microbial targets act as blood flow markers and non-specific uptake indicators.

Fig. 1 presents the biodistribution for ^{99m}Tc-Antibac1 and the ^{99m}Tc-library in the *S. aureus*-infected mice. The results showed a higher uptake of the ^{99m}Tc-Antibac1 in the infected thigh compared to the radiation measured in the left thigh muscle. The target to non-target (T/NT) ratio was of 3.2 ± 0.2. This ratio was statistically higher ($p < 0.05$) than that found for the ^{99m}Tc-library (1.5 ± 0.1). The biodistribution in the fungal-infected model is shown in Fig. 2. No statistical difference ($p > 0.05$) was observed between ^{99m}Tc-Antibac1 and ^{99m}Tc-library. The T/NT ratios were of 1.5 ± 0.1 and 1.5 ± 0.2, respectively, indicating non-specificity of ^{99m}Tc-Antibac1 to *C. albicans* focus.

Blood clearance of ^{99m}Tc-Antibac1 is shown in Fig. 3. The radiolabeled aptamer decays in a biphasic manner, showing a distribution half-life of 6.7 min and an elimination half-life of 41.3 min. The ^{99m}Tc-Antibac1 circulate fast and it was quickly cleared from the blood, as reported for many aptamers [5].

The scintigraphic images of *S. aureus*-infected mice showed a visible uptake of ^{99m}Tc-Antibac1 in the infected right thigh at 1.5 and 3.0 h (Fig. 4A). In contrast, when ^{99m}Tc-library (control) was

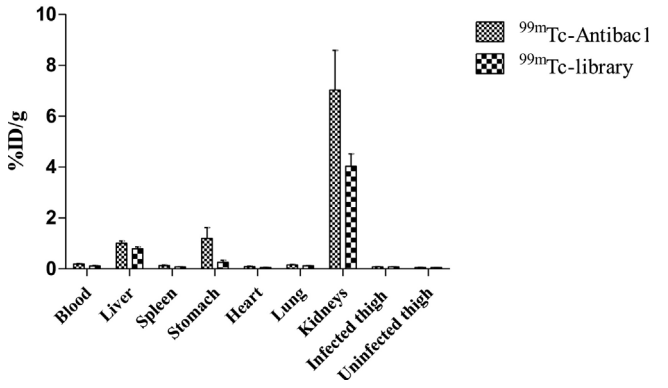

Fig. 2. ^{99m}Tc-Antibac1 and ^{99m}Tc-library biodistribution in the *C. albicans* infection model.
The Antibac1 and the library were labeled with ^{99m}Tc and injected into the tail vein. The mice (n = 6) were euthanized at 3 h after injection, tissue samples were dissected and their activities were measured in a gamma counter.

used, no difference was observed between both thighs (Fig. 4B). The T/NT ratios determined by ROI analysis for ^{99m}Tc-Antibac1 were of 4.7 ± 0.9 and 4.6 ± 0.1 at 1.5 and 3.0 h, respectively. These values were statistically higher ($p < 0.05$) than those found for the ^{99m}Tc-library: 1.6 ± 0.4 and 1.7 ± 0.4, respectively (Fig. 5).

For *C. albicans* infected groups, scintigraphic images of ^{99m}Tc-Antibac1 (Fig. 6A) and the ^{99m}Tc-library (Fig. 6B) were similar. Showing no specific uptake in the infected tight. These findings were corroborated by the low T/NT ratios achieved, at 1.5 and 3.0 h, for ^{99m}Tc-Antibac1 (2.0 ± 0.3 and 2.0 ± 0.6, respectively) and ^{99m}Tc-library (2.1 ± 0.3 and 1.9 ± 0.6, respectively) (Fig. 7). Additionally, the T/NT ratios for ^{99m}Tc-Antibac1 in the *S. aureus*-infected mice were statistically higher ($p < 0.05$) than those attained in the *C. albicans*-infected group (Fig. 8).

The scintigraphic image profiles indicates the urinary tract as the main route of radiotracer elimination since the animals of all groups showed a high uptake in the bladder. No accumulation of radioactivity was observed in thyroid and stomach, indicating acceptable levels of radiochemical impurities.

4. Discussion

Our findings point out a main renal excretion pathway for the ^{99m}Tc-Antibac1 complex, as expected in view of the aptamer features. Aptamers, such as Antibac1, are small (<50 kDa), hydrophilic and negatively charged molecules that allow them

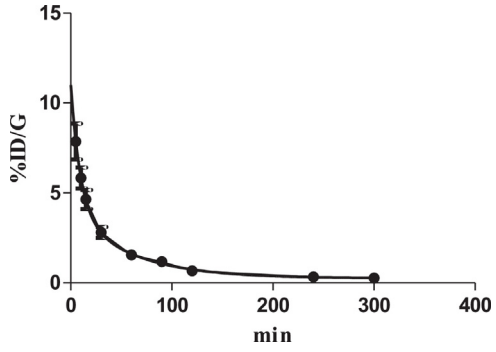

Fig. 3. Blood clearance of ^{99m}Tc-Antibac1.
The ^{99m}Tc-Antibac1 was administrated through the tail vein in a group of six mice. Blood samples (20 μL) were collected at 5, 10, 15, 30, 60, 90, 120, and 240 min after administration. The results were expressed as a percentage of injected activity per gram (%ID/g). The distribution half-life was 6.7 min and elimination half-life was 41.3 min.

to be excreted in a fast and easy way through the renal clearance pathway. The elimination through the renal rout is preferred for radiopharmaceuticals over the hepatobiliary clearance, which presents a slow gastrointestinal transit. However, ^{99m}Tc-Antibac1 showed an elimination half-life of 41.3 min, higher than expected for hydrophilic molecules with similar molecular weight (17.32 kDa) which is far below the molecular cutoff of the renal glomerulus. This result might be explained by a significant percentage of ^{99m}Tc-Antibac1 binding to plasma proteins that delays its glomerular filtration and urinary excretion [10]. The negative charge of ^{99m}Tc-Antibac1 may favor plasma protein binding since most of them are positively charged [11]. Some studies have already shown that oligonucleotides can circulate in bloodstream with a high level of protein binding, such as albumin and α2-macroglobulin [12,13]. Nevertheless, the elimination half-life of 41.3 min seems to be helpful since it prevents very fast ^{99m}Tc-Antibac1 clearance, which can be disadvantageous for imaging since the radiotracer will not be able to accumulate properly.

It is still puzzling to produce imaging probes able to distinguish between infection and inflammation foci since septic focus always presents a certain level of inflammation. The challenges regarding scintigraphic infection imaging are to distinguish between infection and inflammation and selectively distinguish between different types of infection for choosing the correct therapy. Specifically for bacterial infection diagnosis, any radiopharmaceutical commercially available is capable of recognizing directly the presence of the bacteria. Due to the local inflammatory process that often accompanies infection, many radiopharmaceuticals might lead to false-positive outcomes as a result of their leakage from capillaries [1]. Promising results in this area have been obtained with radiolabeled antimicrobial peptides. Antimicrobial peptides are an important component of the innate immune system that provides protection against microbial attacks. Several successful clinical studies have been reported using the radiolabeled ubiquicidin peptide for imaging infection [14]. The radiolabeled leukocytes are still considered the gold standard procedure for the diagnosis of joint prosthesis, endocarditis, inflammatory bowel diseases and osteomyelitis [15]. However, despite presenting specificity for infection, these radiotracers are unable to identify which microorganism is causing the infection. The rationale to use aptamers for infection diagnosis is that they can bind specifically to microorganisms and might be capable of distinguishing infection from aseptic inflammation and identify the microorganism as well.

A radiolabeled library was used as a control for monitoring nonspecific uptake at the site of infection. The library is made of oligonucleotides in similar size than Antibac1 but with random sequences. The library was radiolabeled in the same way as Antibac1. As the oligonucleotides of the library do not have specificity for the microbial cells, the discrete uptake in the infection foci for both experimental models (*S. aureus* and *C. albicans*) is likely due to the increased capillary permeability and vasodilatation caused by the associated inflammation. Nevertheless, high ^{99m}Tc-Antibac1 uptake in the *S. aureus* infection foci was verified in the biodistribution and scintigraphic imaging assays. A significant increase in the T/NT ratio was observed for ^{99m}Tc-Antibac1 in comparison to ^{99m}Tc-library, indicating the feasibility of ^{99m}Tc-Antibac1 in detecting the bacterial infection. In contrast, for the *C. albicans*-infected animals, in which ^{99m}Tc-Antibac1 has no affinity, T/NT ratios were similar to that observed for the ^{99m}Tc-library.

Aptamers are promising tools in nuclear medicine and they have advantages to other biomolecules as radiopharmaceuticals. They seem to be non-toxic and non-immunogenic, have small size (10 to 20 kDa) and fast clearance. Aptamers can be selected for almost any target, including toxic and non-imunogenic molecules.

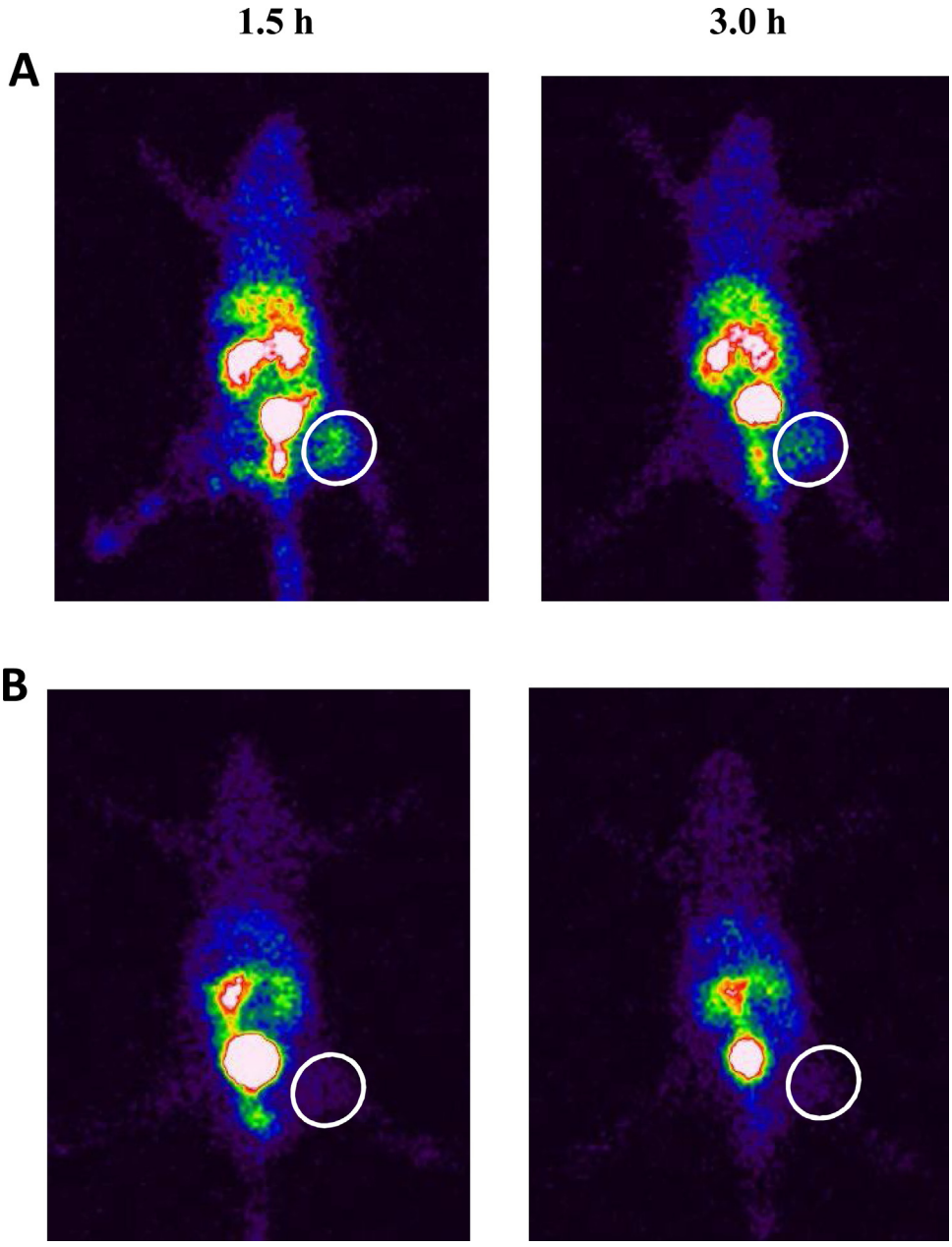

Fig. 4. Scintigraphic images of *S. aureus*-infected mice.
The figures show representative images of *S. aureus*-infected mice. Six animals were imaged per group. (A) Mice that received the ^{99m}Tc-Antibac1. (B) Mice that received the ^{99m}Tc-library. The circles indicate the infectious foci.

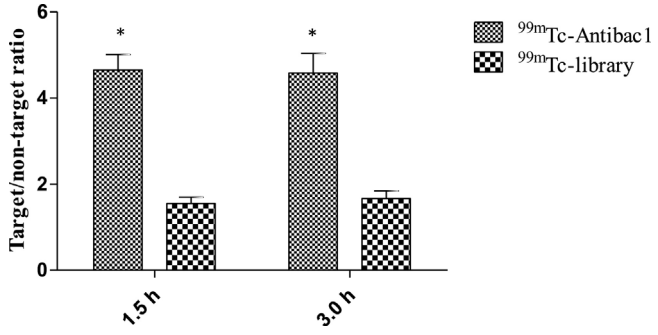

Fig. 5. Target to non-target ratios determined by ROI for the ^{99m}Tc-Antibac1 and the ^{99m}Tc-library in the *S. aureus* infected group at 1.5 h and 3.0 h.
The ratios of the count in the target to non-target ROI were calculated using the total counts. The symbol (*) indicates statistical difference in relation to the control (^{99m}Tc-library) ($p < 0.05$). Six mice were imaged per group.

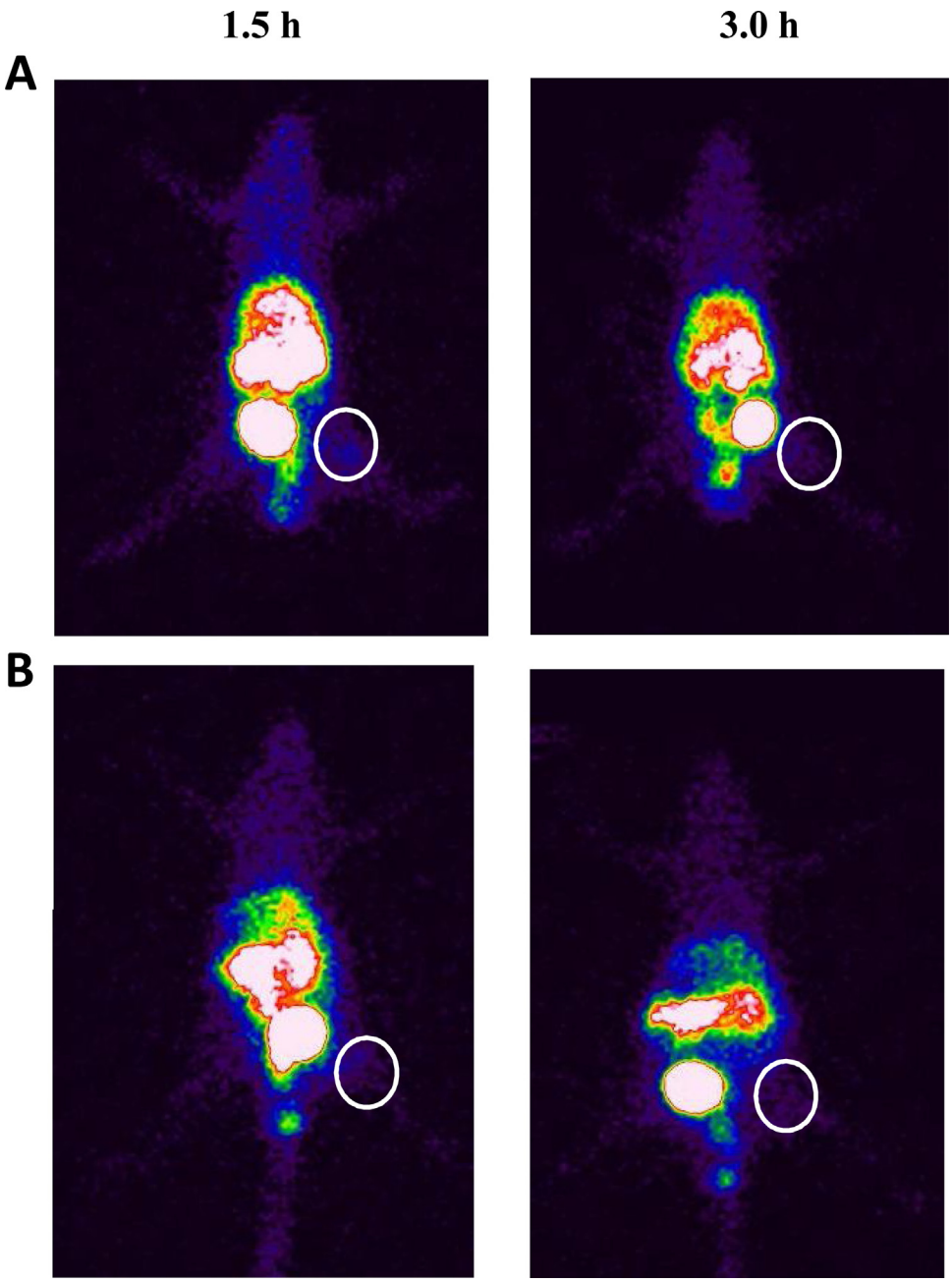

Fig. 6. Scintigraphic images of *C. albicans*-infected mice.
The figures show representative images of *C. albicans*-infected mice. Six animals were imaged per group. (A) Mice that received the ^{99m}Tc-Antibac1. (B) Mice that received the ^{99m}Tc-library. The circles indicate the infectious foci.

Due to their small size and structural flexibility, aptamers may bind hidden epitopes. Aptamers can be easily produced by *in vitro* conditions with high reproducibility and free of contaminants, and the chemical synthesis makes them receptive to many modifications such as to make them more resistant to nucleases or to incorporate chelating groups [16]. Lyophilized aptamers can be stored for years and, once reconstituted; they can be boiled or subjected to many freeze-thaw cycles [17]. Due to the high specificity, large variety of potential targets, and the possibility of labeling with different radionuclides, aptamers have great potential for radiopharmaceuticals development [5]. Radiolabeled aptamers against several cancer-related targets including, nucleolin [18], tenascin-C [19,20], mucin 1 (MUC1) [21], members of the human epidermal growth factor receptor (HER) family [22,23], among others, have been tried in preclinical studies. Radiolabeled aptamers for non-cancer disease imaging have also been reported for thrombus imaging [24], inflammation [25] and infection diagnosis [8,9,26].

Ferreira et al. [6] selected the aptamer Antibac1 by SELEX targeting the peptidoglycan. The Antibac1 dissociation constant (K_d) for peptidoglycan was 0.415 ± 0.047 μM. The radiolabeled Antibac1 showed high binding capacity for *S. aureus* and *E. coli* cells *in vitro*. On the other hand, the binding to *C. albicans* and human fibroblasts was negligible, demonstrating their specificity for bacterial cells. In another study, we also showed that Antibac1 binds with high efficiency to four Gram-positive and seven Gram-negative bacterial species [27]. The dissociation constant determined for *S. aureus* cells was 0.170 ± 0.032 μM. These results encouraged us to evaluate the feasibility of Antibac1 as a scintigraphic imaging probe for bacterial infection diagnosis. In

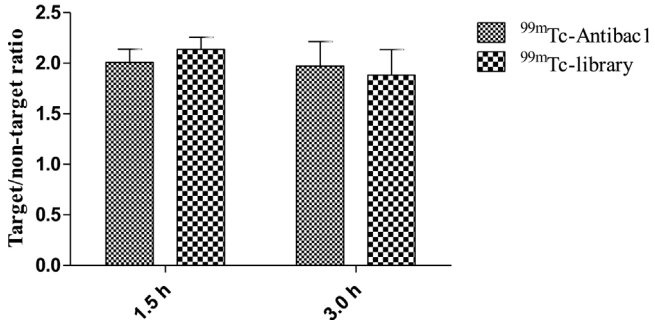

Fig. 7. Target to non-target ratios determined by ROI for the ^{99m}Tc-Antibac1 and the ^{99m}Tc-library in the *C. albicans*-infected group at 1.5 h and 3.0 h.
The ratios of the count in the target to non-target ROI were calculated using the total counts. No statistical difference was verified between the groups ($p > 0.05$). Six mice were imaged per group.

order to explore this hypothesis, Antibac1 was labeled with ^{99m}Tc and scintigraphic images were acquired after injection into bacterial infection-bearing mice. An experimental model of *S. aureus* infection was chosen since this species is closely related to skin, soft tissues, bone and bone prostheses infections [28]. A control group of animals infected with *C. albicans* was used to measure the aptamer specificity for bacterial infection. The results demonstrated that the ^{99m}Tc-Antibac1 was effective to identify a bacterial infection focus and to distinguish it from a fungal one.

5. Conclusions

The peptidoglycan aptamer Antibac1 was successfully labeled with ^{99m}Tc, showing high stability for *in vivo* imaging. In a *S. aureus*-infected model, the T/NT ratios for ^{99m}Tc-Antibac1 were substantially higher than the control group. However, ratios were similarly low when a *C. albicans*-infected model was tested. These findings suggested that the ^{99m}Tc-Antibac1 is a feasible imaging probe to identify a bacterial infection focus. In addition, this radiolabeled aptamer seems to be suitable in distinguishing between bacterial and fungal infection.

Conflicts of interests

Authors declare that they have no conflict of interest.

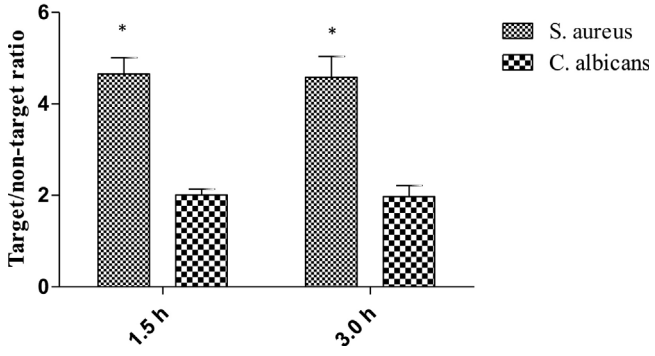

Fig. 8. Comparison of the target to non-target ratios determined by ROI for ^{99m}Tc-Antibac1 uptake in the *S. aureus*- and the *C. albicans*-infected mice groups.
The symbol (*) indicates statistical difference in the ^{99m}Tc-Antibac1 uptake between the *S. aureus*- and the *C. albicans*-infected mice groups ($p < 0.05$). Six mice were imaged per group.

Author contributions

A.S.R.A, I.M.F and A.L.B.B conceived and designed the experiments; I.M.F., C.M.S.L. and S.R.S. performed the experiments; A.S.R.A, A.L.B.B, V.N.C. and S.O.F analyzed the data; A.S.R.A and I.M.F wrote the paper.

Acknowledgement

This research was supported by Fundação de Amparo à Pesquisa do Estado de Minas Gerais (FAPEMIG) (TEC-APQ-02247-16).

References

[1] G. Ferro-Flores, B.E. Ocampo-Garcia, L. Melendez-Alafort, Development of specific radiopharmaceuticals for infection imaging by targeting infectious micro-organisms, Curr. Pharm. Des. 18 (2012) 1098–1106.
[2] C. Tsopelas, Radiotracers used for the scintigraphic detection of infection and inflammation, ScintificWorldJournal (2015), doi:http://dx.doi.org/10.1155/2015/676719.
[3] A.D. Ellington, J.W. Szostak, In vitro selection of RNA molecules that bind specific ligands, Nature 346 (1990) 818–822.
[4] C. Tuerk, L. Gold, Systematic evolution of ligands by exponential enrichment: RNA ligands to bacteriophage T4 DNA polymerase, Science 249 (1990) 505–510.
[5] M. Gijs, A. Aerts, N. Impens, S. Baatout, A. Luxen, Aptamers as radiopharmaceuticals for nuclear imaging and therapy, Nucl. Med. Biol. 43 (2016) 253–271.
[6] I.M. Ferreira, C.M. Sousa Lacerda, L.S. Faria, C.R. Corrêa, A.S.R. Andrade, Selection of peptidoglycan-specific aptamers for bacterial cells identification, Appl. Biochem. Biotechnol. 174 (2014) 2548–2556.
[7] C.R. Correa, A.L.B. de Barros, C.A. Ferreira, A.M. Goes, V.N. Cardoso, A.S.R. Andrade, Aptamers directly radiolabeled with technetium-99m as a potential agent capable of identifying carcinoembryonic antigen (CEA) in tumor cells T84, Bioorg. Med. Chem. Lett. 24 (2014) 1998–2001.
[8] S.R. dos Santos, C.R. Corrêa, A.L. Branco de Barros, R. Serakides, S.O. Fernandes, V.N. Cardoso, A.S.R. de Andrade, Identification of *Staphylococcus aureus* infection by aptamers directly radiolabeled with technetium-99m, Nucl. Med. Biol. 42 (2015) 292–298.
[9] C.M. de Sousa Lacerda, I.M. Ferreira, S.R. Santos, A.L.B. Barros, S.O. Fernandes, V. N. Cardoso, A.S.R. Andrade, (1 → 3)-β-D-glucan aptamers labeled with technetium-99m: biodistribution and imaging in experimental models of bacterial and fungal infection, Nucl. Med. Biol. 46 (2017) 19–24.
[10] C.K. Younes, R. Boisgard, B. Tavitian, Labelled oligonucleotides as radiopharmaceuticals: pitfalls, problems and perspectives, Curr. Pharm. Des. 6 (2002) 1451–1466.
[11] S.P. Henry, M. Johnson, T.A. Zanardi, R. Fey, D. Auyeung, P.B. Lappin, A.A. Levin, Renal uptake and tolerability of a 2′-O-methoxethyl modified antisense oligonucleotide (ISIS 113715) in monkey, Toxicology 301 (2012) 13–20.
[12] D.A. Brown, S.H. Kang, S.M. Gryaznov, L. DeDionísio, O. Heidenreich, S. Sullivan, X. Xu, M.I. Nerenberg, Effect of phosphorothioate modification of oligodeoxynucleotides on specific protein binding, J. Biol. Chem. 269 (1994) 26801–26805.
[13] S.K. Srinivasan, H.K. Tewary, P.L. Iversen, Characterization of binding sites extent of binding, and drug interactions of oligonucleotides with albumin, Anti-Sense Res. Dev. 5 (1995) 131–139.
[14] A. Ostovar, M. Assadi, K. Vahdat, I. Nabipour, H. Javadi, M. Eftekhari, M. Assadi, A pooled analysis of diagnostic value of ^{99m}Tc-ubiquicidin (UBI) scintigraphy in detection of an infectious process, Clin. Nucl. Med. 38 (2013) 413–416.
[15] J. Dutta, T. Naicker, T. Ebenhan, H.G. Kruger, P.I. Arvidsson, T. Govender, Synthetic approaches to radiochemical probes for imaging of bacterial infections, Eur. J. Med. Chem. 133 (2017) 287–308.
[16] S. Missailidis, A. Perkins, Update: aptamers as novel radiopharmaceuticals: their applications and future prospects in diagnosis and therapy, Cancer Biother. Radiopharm. 22 (2007) 453–468.
[17] C. Evtugyn, A. Porfireva, V. Stepanova, R. Sitdikov, I. Stoikov, D. Nikolelis, T. Hianik, Electrochemical aptasensor based on polycarboxylicmacrocycle modified with neutral red for aflotoxin B1 detection, Electroanalysis 26 (2014) 2100–2109.
[18] W. Hwang, H.Y. Ko, J.H. Lee, H. Kang, S.H. Ryu, I.C. Song, D.S. Lee, S. Kim, A nucleolin-target multimodal nanoparticle imaging probe for traking cancer cells using an aptamer, J. Nucl. Med. 51 (2010) 98–105.
[19] B.J. Hicke, A.W. Stenphens, T. Gould, Y.F. Chang, C.K. Lynott, J. Heil, S. Borkowski, C.S. Hilger, G. Cook, S. Warren, P.G. Schmidt, Tumor targeting by an aptamer, J. Nucl. Med. 47 (2006) 668–678.
[20] B.K.R. Boisgard, B. Jego, K. Siquier, F. Hinnen, F. Dollé, M. Friebe, S. Borkowski, L. Dinkelborg, B. Tavitian, In vivo PET tumor imaging using an [F18] labelled aptamer targeting tenascin-C, J. Nucl. Med. 50 (2009) 1594.
[21] C.D. da Pieve, A.C. Perkins, S. Missailidis, Anti-MUC1 aptmers: radiolabelling with (99m)Tc and biodistribution in MCF-7 tumor-bearing mice, Nucl. Med. Biol. 36 (2009) 703–710.

[22] K. Varmira, S.J. Hosseinimehr, Z. Noaparast, S.M. Abedi, An improved radiolabelled RNA aptamer molecule for HER2 imaging in cancer, J. Drug. Target 22 (2014) 116–122.
[23] X. Wu, H. Liang, Y. Tan, C. Yuan, S. Li, X. Li, G. Li, Y. Shi, X. Zhang, Cell-SELEX aptamer for highly specific radionuclide molecular imaging of gioblastoma in vivo, PLoS One 9 (2014) e90752.
[24] H. Dougan, J.I. Weitz, A.R. Stafford, K.D. Gillespie, P. Klement, J.B. Hobbs, D.M. Lyster, Evaluation of DNA aptamers directed to thrombin as potential thrombus imaging agents, Nucl. Med. Biol. 30 (2003) 61–72.
[25] J. Charlton, J. Sennello, D. Smith, In vivo imaging of inflammation using an aptamer inhibitor of human neutrophil elastase, Chem. Biol. 4 (1997) 809–816.
[26] S.R. dos Santos, C.M. de Sousa Lacerda, I.M. Ferreira, A.L.B. Barros, S.O. Fernandes, V.N. Cardoso, A.S.R. Andrade, Scintigraphic imaging of Staphylococcus aureus infection using ^{99m}Tc radiolabeled aptamers, Appl. Radiat. Isot. 128 (2017) 22–27.
[27] A.C. Graziani, M.I. Stets, A.L. Lopes, P.H. Schluga, S. Marton, I.F. Mendes, A.S.R. Andrade, M.A. Krieger, J. Cardoso, High efficiency binding aptamers for a wide range of sepsis bacterial agents, J. Microbiol. Biotechnol. 27 (4) (2017) 838–843.
[28] F. Gemmel, V. Wyngaert, C. Love, M. Welling, P. Gemmel, C. Palestro, Prosthetic joint infections: radionuclide state-of-the-art imaging, Eur. J. Nucl. Med. Mol. Imaging 39 (2012) 892–909.